



## Original article

## Examining the intrinsic foot muscles' capacity to modulate plantar flexor gearing and ankle joint contributions to propulsion in vertical jumping

Ross Smith<sup>a,\*</sup>, Glen Lichtwark<sup>a</sup>, Dominic Farris<sup>b</sup>, Luke Kelly<sup>a</sup><sup>a</sup> School of Human Movement and Nutrition Sciences, The University of Queensland, Brisbane, QLD 4072, Australia<sup>b</sup> Sport and Health Sciences, College of Life and Environmental Sciences, The University of Exeter, Exeter, EX1 2LU, United Kingdom

Received 21 October 2021; revised 8 March 2022; accepted 16 June 2022

2095-2546/© 2022 Published by Elsevier B.V. on behalf of Shanghai University of Sport. This is an open access article under the CC BY-NC-ND license. (<http://creativecommons.org/licenses/by-nc-nd/4.0/>)**Abstract**

**Background:** During human locomotion, a sufficiently stiff foot allows the ankle plantar flexors to generate large propulsive powers. Increasing foot stiffness (e.g., via a carbon plate) increases the ankle's external moment arm in relation to the internal moment arm (i.e., increasing gear ratio), reduces plantar flexor muscles' shortening velocity, and enhances muscle force production. In contrast, when activation of the foot's intrinsic muscles is impaired, there is a reduction in foot and ankle work and metatarsophalangeal joint stiffness. We speculated that the reduced capacity to actively control metatarsophalangeal joint stiffness may impair the gearing function of the foot at the ankle.

**Methods:** We used a tibial nerve block to examine the direct effects of the intrinsic foot muscles on ankle joint kinetics, *in vivo* medial gastrocnemius' musculotendinous dynamics, and ankle gear ratio on 14 participants during maximal vertical jumping.

**Results:** Under the nerve block, the internal ankle plantar flexion moment decreased ( $p = 0.004$ ) alongside a reduction in external moment arm length ( $p = 0.021$ ) and ankle joint gear ratio ( $p = 0.049$ ) when compared to the non-blocked condition. Although medial gastrocnemius muscle–tendon unit and fascicle velocity were not different between conditions, the Achilles tendon was shorter during propulsion in the nerve block condition ( $p < 0.001$ ).

**Conclusion:** In addition to their known role of regulating the energetic function of the foot, our data indicate that the intrinsic foot muscles also act to optimize ankle joint torque production and leverage during the propulsion phase of vertical jumping.

**Keywords:** Ankle biomechanics; Ankle gearing; Foot biomechanics

**1. Introduction**

When running and walking, the ankle plantar flexors produce more average positive power than the larger, more proximal muscles acting around the hip and knee.<sup>1</sup> A substantial proportion of this power is delivered via elastic recoil of the Achilles tendon during propulsion.<sup>2,3</sup> It appears the foot plays an important role in modulating the behavior of the ankle plantar flexors and Achilles tendon by acting as a lever with a constantly varying length throughout the stance phase. This function acts to alter the ratio of external moment arm to internal moment arm at the ankle joint, also known as the gear ratio.<sup>4</sup> This dynamic gearing is potentially associated with the optimization of shortening velocities of the ankle plantar flexor muscle–tendon unit (MTU), improving force production and

positive power output during walking and running.<sup>5,6</sup> Simulations also suggest variable gearing may enable supramaximal ankle power outputs, where relatively short heels (shorter internal moment arm) and long feet/toes (longer external moment arm) would allow increased terminal gear ratio and slow MTU shortening speeds during sprinting propulsion.<sup>7</sup>

*In vivo* studies have also sought to elucidate the relationship between foot and ankle contributions to locomotion. Takahashi et al.<sup>8</sup> examined the effects of modulating the stiffness of the foot/shoe complex during walking, via the addition of a carbon fiber plate inside a shoe. Increased foot stiffness (delivered from the carbon fiber plate) resulted in increased soleus force and reduced soleus shortening velocities.<sup>8</sup> The increased foot stiffness delivered from the carbon plate also resulted in an increased ankle plantar flexor gear ratio, which was largely driven by an increase in external moment arm length during propulsion.<sup>8</sup> Willwacher et al.<sup>9</sup> have previously reported similar findings during running with carbon fiber shoe inserts.

Peer review under responsibility of Shanghai University of Sport.

\* Corresponding author.

E-mail address: [ross.smith1@uq.net.au](mailto:ross.smith1@uq.net.au) (R. Smith).

<https://doi.org/10.1016/j.jshs.2022.07.002>

Thus, externally stiffening the foot appears to increase the external ankle joint moment arm length and ankle gear ratio, which may act to improve muscle contractile dynamics, potentially enhancing force and power output.

The plantar intrinsic foot muscles (IFM), located within the arch of the human foot, also appear to play an important role in modulating the mechanical function of the foot. Together with the extrinsic foot muscles, these muscles modulate metatarsophalangeal joint (MTPj) stiffness during propulsion,<sup>10,11</sup> as well as modulate both energy absorption and generation through the foot in a diverse array of locomotion tasks.<sup>10,12–14</sup> The potential importance of the IFM for human athletic performance has been widely argued.<sup>15–18</sup> However, there is little evidence that stronger IFM can actually enhance performance. To our knowledge, a single study by Goldmann et al.<sup>18</sup> reported increased strength of the IFM was associated with increased horizontal jump performance and no changes in walking, running, or vertical jump performance. Also, the IFM have been shown to alter the position of the center of pressure, relative to the ankle joint, upon activation.<sup>19</sup> Therefore, it is plausible that these muscles may contribute to the dynamic gearing function of the foot around the ankle by modulating external moment arm length. This mechanism may explain why we have observed reductions in ankle joint work and plantar flexion torque when the active force production from the IFM is temporarily removed via anaesthesia.<sup>10,12</sup>

Thus, the aim of this study was to determine the contribution of the IFM to the gearing function of the foot around the ankle, as well as the impact on ankle joint kinetics and plantar flexor muscle–tendon behavior during maximal effort unilateral jumping. In contrast to previous investigations of walking and running,<sup>10</sup> a maximal effort task was performed before and after the application of a tibial nerve block to see how removing IFM contributions affected positive work generation capacity of the lower limb system when jumping (i.e., foot, ankle, knee, hip contributions). We hypothesized that the absence of active force production from the IFM would lead to a reduction in external ankle joint moment arm length, due to the absence of active MTPj stiffening and reduced anterior translation of the center of pressure relative to the ankle joint. Further, we hypothesized that these alterations would produce an increase in ankle plantar flexor fascicle velocity and a reduction in ankle plantar flexion torque and positive power.

## 2. Methods

### 2.1. Participants

We recruited 16 recreationally active individuals (12 males and 4 females,  $29.4 \pm 11.8$  years (mean  $\pm$  SD),  $1.73 \pm 0.22$  m,  $73.7 \pm 17.8$  kg) to participate in this study. Two males were excluded from all fascicle and MTU variable analyses due to complications with accurately measuring their fascicle images, and an additional 2 males were excluded altogether from analysis due to inadequate motor nerve blocks. Thus, for all MTU and fascicle analyses, 12 participants were included, and for the

remaining analyses, 14 participants were included. All participants provided written informed consent to participate, and this study was approved by the ethics committee at the University of Queensland in accordance with the Declaration of Helsinki.

### 2.2. Protocol

Following a series of familiarization trials, participants performed 5 unilateral maximal effort jumps from their dominant foot. All participants were encouraged to jump with maximal intent and were able to land any way they desired, to remove any potential distractions. Following the completion of the 5 jumps, a peripheral nerve block was applied at the level of the medial malleolus to temporarily remove the active force-producing capacity of the plantar IFM (see Section 2.3). Once a successful nerve block was achieved, the unilateral jumping protocol was repeated. Due to the limitations in local anaesthesia dosage, only 1 foot could be anaesthetized. Thus, the choice of unilateral instead of bilateral jumps was made to ensure the validity of our repeated measures design by eliminating potential compensatory action by the non-blocked limb. Due to the balance constraints imposed by unilateral jumping, the use of arms for balance and swing during the jumps' countermovement were allowed. A successful trial was 1 where the participant assumed a unilateral stance on their jumping leg and where the non-jumping leg did not come in contact with the ground during the countermovement and propulsive phases.

### 2.3. Tibial nerve block

A tibial nerve block was administered through injection of a 2% lignocaine plain solution (2% Xylocaine; AstraZeneca, New South Wales, Australia) at the tibial nerve, approximately (2–4 cm) proximal to the medial malleolus.<sup>10</sup> The injection site was guided by ultrasound to determine the location of the tibial nerve and ensure the accuracy and safety of the procedure. Because the maximum dose was restricted to 3 mg/kg of body mass, the block was applied only to the dominant foot to ensure the quality of anaesthesia coverage and participant safety. For all participants, confirmation of a complete motor block was ensured by monitoring the electromyography (EMG) signal from a pair of surface electrodes with a 20-mm inter-electrode distance (Tyco Healthcare Group, Neustadt, Germany) placed on the plantar surface of the medial longitudinal arch during a toe plantar flexion maximal voluntary contraction. To establish a reference signal amplitude, the EMG signal was recorded during a series of maximal effort toe flexion tasks, performed immediately prior to the administration of the block. The EMG signal amplitude was then checked repeatedly following administration of the nerve block until we observed a reduction of 90% or greater in arch muscle activation amplitude when compared to the reference value. We ensured an efficacious block throughout our task completion by checking the arch muscle EMG signal at the end of the protocol.

## 2.4. Data collection and processing

### 2.4.1. Kinematics and kinetics

Motion capture data was collected using a 14-camera system (Oqus; Qualisys, Gothenburg, Sweden) at 125 Hz or 250 Hz. This discrepancy was due to some inconsistencies in reflective-marker recognition at the lower capture rate (125 Hz) for participants tested early in recruitment, which was remedied by doubling the capture rate. Ground reaction force data was sampled at 1250 Hz (AMTI, Watertown, MA, USA). Reflective markers (6.4 mm; B&L Engineering, Santa Ana, CA, USA) were placed on the following bony landmarks to generate rigid segments for the pelvis, femur, and shank respectively: left and right anterior superior iliac spine and posterior superior iliac spine on the pelvis, medial and lateral epicondyles on the femur, as well as medial and lateral malleoli on the shank. Rigid clusters of 4-marker were secured to the shank and thigh to track the motion of each segment during the jumping tasks. Markers were placed on the foot in accordance with a modified Rizzoli multi-segment foot model<sup>20</sup> to track the motion of the calcaneus, metatarsals, and toe segments. Ankle joint angles were defined as rotation of the calcaneus about the shank, while MTPj angles were defined as rotation of the toe segment about the metatarsals. A static calibration trial was collected in order to establish segment dimensions. Marker data for the pelvis, femur, shank, calcaneus, metatarsal, and toes segments were used to construct an inverse kinematic model within Visual 3D (C-Motion Inc, Germantown, MD, USA). Inverse kinematics for motion data were calculated using a pelvis to thigh, thigh to shank, shank to foot (calcaneus), and metatarsal to toes chain. The knee and ankle were modeled with 3 degrees of freedom to allow angular rotation (flexion/extension, abduction/adduction, and internal/external rotation), with translations excluded. The hip joint and MTPj were modeled as traditional six-degree-of-freedom joints. For each frame, the inverse kinematic model optimized a new skeletal pose ( $q$ ) for defined segments by solving a weighted least squares problem to minimize the difference between marker data coordinates ( $r$ ) and model-based coordinates ( $f$ ) for each segment,<sup>21,22</sup> whose notation is shown below:

$$F(q) = \sum_{i=1}^M \|r_i - f_i(q)\|^2,$$

where  $r$  is body segment position (X, Y, and Z) and  $f$  is a known function of  $q$  where marker  $i$  is placed at a known position ( $p$ ) and orientation ( $R$ ) within the segment's reference frame:

$$r_i = r(q) + R(q) \times p_i = f_i(q).$$

A weighted solution is necessary for a whole-model solution, as segments with larger residual tracking errors due to soft tissue artifact (e.g., thigh) will influence the minimization solution for other segments. For our solution, all segments were weighted equally except for the shank and calcaneus, which were doubly weighted to correct for soft tissue artifact.<sup>22</sup> All joint rotations were expressed in relation to the proximal segment. Joint rotation polarity and Cardan rotational sequence was determined by

a right-hand rule for all tri-dimensional angular computations where X is the longitudinal axis, Y is the anteroposterior axis, and Z is the mediolateral axis.

We examined the effect of the nerve block over the propulsive phase of the jump, which was defined as the period from the bottom of the jumping countermovement (start) until the point that vertical ground reaction force subsided below 25% of its peak value (end). The start event was defined as the point at which the center of mass (COM) velocity (see Section 2.5.1 for details) passed through zero from negative to positive. We selected our end event for the following 2 reasons: First, during the period immediately before take-off, the quality of muscle fascicle images is drastically reduced, increasing the error in tracking fascicle lengths and velocities during this time. Second, during the same period just prior to take-off, center of pressure measurements are noisy at low force levels, creating inaccuracies in external moment arm lengths, and thus, ankle joint gear ratios (which has also been reported by Willwacher et al.<sup>9</sup> Thus, the 25% cut-off in vertical ground reaction force is arbitrary, as it is based on visual inspection of the gearing data, but its use enables confidence in the accuracy of our ultrasound and gearing measures while still retaining the period over which the largest kinetic output of the ankle was performed.

### 2.4.2. Muscle–tendon function

Ultrasound data for the medial gastrocnemius (MG) were collected by placing a 128-element flathead ultrasound transducer (LV 7.5/60/128Z-2; Telemed, Vilnius, Lithuania) over the muscle tissue and recorded by a PC-based ultrasound system (ArtUs EXT-1H, Telemed). Upon obtainment of a high-quality image, the transducer was fixed at that site and secured using self-adhesive tape such that the transducer would not slip out of the plane in which fascicles shortened.<sup>23</sup> Caution was taken to ensure that the tape was secured with an even pressure but was not made excessively tight in order to avoid affecting the muscle geometry within the image.<sup>24</sup> Ultrasound data were sampled between 95–168 Hz to capture rapid changes in fascicle length. In some cases at the lower ends of our range of capture rates, we were forced to sacrifice our capture framerate to raise the image quality. The ultrasound sampling rate was held constant within each participant.

### 2.4.3. Muscle activation

EMG data for the MG and tibialis anterior (TA) were amplified by 1000, and then band-pass filtered at a bandwidth of 30–500 Hz (MA300; Motion Lab Systems, Baton Rouge, LA, USA) and sampled at 4000 Hz by a 14-bit analog-to-digital converter (Qualisys). The initial hardware filter was used to ensure the quality of EMG data in real time, as it is monitored throughout collection. Bi-polar surface electrodes (MA310; Motion Lab Systems) were secured with self-adhesive tape just medially to the central portion of the MG muscle belly and in line with the central portion of the TA. Each muscle's electrodes were placed as close to the muscle belly as possible

and oriented such that the electrodes' long axis was parallel to the muscle fibers' orientation. This placement was chosen to minimize cross-talk from other ankle plantar flexor muscles while accommodating the presence of the ultrasound transducer occupying the MG's most central portion.

## 2.5. Data analysis

### 2.5.1. COM and MTPj mechanics

Peak vertical ground reaction force was calculated during the propulsive phase (defined in Section 2.4.1) for all jumps across both conditions. Vertical jump height was calculated using the terminal velocity at take-off, the height of the COM at take-off, and equations of uniform accelerated motion. Velocity of the COM was first calculated based on the cumulative time integral of acceleration (vertical ground reaction force minus body weight/body mass) from start of the downward movement to the time that the ground reaction force went to zero. Displacement of the COM was then determined relative to the start position by calculating the cumulative time integral of the velocity. Finally, jump height was calculated by adding the height gained during aerial phase (take-off-velocity<sup>2</sup>/(2 × gravity)) to the displacement at take-off.

MTPj quasi-stiffness was calculated as the absolute value of the peak MTPj moment divided by the change in MTPj angle from MTPj start until peak MTPj moment. The MTPj moment was calculated as a net internal moment, using a Newtonian–Euler approach. MTPj start was the time-point at which the MTPj moment crossed zero to become an internal plantar flexion moment, which is synonymous with the ground reaction force shifting anteriorly to the joint's rotational axis. This step is necessary to ensure the moment attributed to the joint is valid based on the limitations of inverse dynamic calculations within the foot segments.<sup>25,26</sup>

### 2.5.2. Ankle joint mechanics

Ankle joint gear ratio was calculated as the ratio of the lengths of the external moment arm and the internal moment arm over the propulsive phase. The external moment arm length was calculated as the 2D-perpendicular distance between the ankle joint center and the projected vector of the ground reaction force in the sagittal (Z and Y) plane, and the internal moment arm was calculated as the perpendicular distance between the ankle joint center and a line created by a longitudinal projection along the shank from the calcaneus marker to a virtual landmark set at half of shank length. The ankle joint plantar flexion moment is reported as a net internal moment, using a Newtonian–Euler approach. All relative segment masses, joint centers, COM locations, and moments of inertia were Visual 3D defaults.<sup>27,28</sup> Ankle joint power was calculated as the dot product of the sagittal plane ankle joint moment and ankle joint angular velocity.

### 2.5.3. Muscle–tendon function

The MG MTU length and velocity during the propulsive phase were calculated according to a previously reported regression equation<sup>29</sup> using ankle and knee joint kinematics.

Fascicle lengths of the MG muscle during the jumping tasks were obtained using a previously described semi-automatic tracking algorithm.<sup>30,31</sup> This algorithm implements an affine extension to an optic flow algorithm to track movement of muscle fascicle end-points throughout dynamically recorded sequences of ultrasound images. Muscle fascicle length was defined as the instantaneous distance between the deep and superficial aponeuroses along a clearly defined fascicle. Mean fascicle velocity was calculated as net length change throughout propulsion. MG tendinous tissue length was calculated as MTU length minus the dot product of fascicle length and the cosine of the pennation angle.<sup>32</sup>

### 2.5.4. Muscle activation

Muscle activation data during the propulsive phase were processed using a custom Matlab script (MathWorks, Natick, MA, USA). EMG signals were high-pass filtered using a second-order Butterworth filter at 35 Hz, rectified, and low-pass filtered using a second-order Butterworth filter at 10 Hz to generate an EMG envelope.<sup>33</sup> The final low-pass filter is performed to relate muscle activation data to the movement frequency, where 10 Hz adequately captures the highest movement frequencies we would see during jumping. These data were normalized to each subject's peak value for that muscle across all trials for all tasks, then averaged across trials within each subject.

## 2.6. Statistics

Two-tailed statistical parametric mapping paired *t* tests were performed in Matlab using the *spm1d*<sup>34</sup> (Version M.0.4.7; www.spm1d.org) to assess the effect of the nerve block on ankle gearing, ankle kinetics, MG MTU and fascicle dynamics, as well as MG EMG. This analysis was selected to identify notable phases for all time-series data throughout jumping propulsion. As the statistical parametric mapping method compares data vectors over the same time period (time normalized), we ensured propulsion times between conditions were not significantly different (2.75% difference, blocked = 0.987 s, non-blocked = 1.015 s; *p* = 0.622). For each comparison, the subject-averaged data per condition was used for statistical comparison. Also, for continuous analyses, we calculated Cohen's *d* at each time point and reported the mean value over the period of each significant effect. This allows estimation of the nerve block intervention's effect; however, this method for continuous analyses may be subject to inflated error in the measurement.<sup>35</sup> A paired sample *t* test (Jamovi, Version 1.6; www.jamovi.org) was performed to assess the effect of the block on vertical jump height and MTPj quasi-stiffness. Alpha for statistical significance for *p* values were set at ≤ 0.05 for all analyses.

## 3. Results

### 3.1. Ground reaction force, jump height, and MTPj mechanics

Mean jump height was significantly lower in the presence of the nerve block as compared to the non-blocked condition

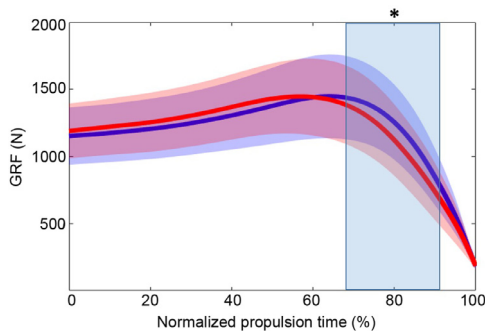


Fig. 1. Group mean data ( $n = 14$ ) for vertical ground reaction force (GRF) in both non-blocked (blue) and blocked (red) conditions. Horizontal brackets represent statistically significant differences between conditions for jump height. Time series data are normalized to the mean trial length from the bottom of the countermovement to 25% of peak vertical GRF. Regions of percent-time with shading and asterisk represent statistically significant differences between conditions ( $p \leq 0.05$ ).

(mean difference =  $0.024 \pm 0.061$  m (mean  $\pm$  SD),  $p = 0.028$ ,  $d = 0.662$ , 95% confidence interval (95%CI): 0.070–1.230). Vertical ground reaction force (Fig. 1) was significantly lower for 67%–92% ( $p < 0.001$ , mean significant Cohen's  $d = 0.376$ ) of the propulsive phase when jumping with the nerve block. MTPj quasi-stiffness decreased substantially in the nerve block condition (mean difference =  $1.2 \pm 0.89$  N  $\times$  degree/kg;  $p < 0.001$ ;  $d = 1.38$ , 95%CI: 0.625–2.110).

### 3.2. Ankle joint mechanics and gearing

Fig. 2 presents group mean ankle joint plantar flexion moment, angular velocity, and power for both conditions during the time-normalized propulsive phase. The application of the nerve block produced a significant decrease in ankle plantar flexion moment ( $p = 0.004$ , mean significant Cohen's  $d = 0.718$ ; Fig. 2A) from 64% to 96% of propulsion. However, we observed no differences in ankle joint angular velocity (Fig. 2B) or ankle joint propulsive power (Fig. 2C) when the nerve block was administered.

Fig. 3 shows group mean internal and external ankle joint moment arm lengths and gear ratio throughout the time-normalized propulsive phase. The internal moment arm length was similar between both conditions for the entire propulsion phase (Fig. 3A). The external moment arm length was shorter in the blocked condition from 85% to 92% of the propulsive phase ( $p = 0.021$ , mean significant Cohen's  $d = 0.168$ ; Fig. 3B), and we saw a reduction in ankle joint gear ratio from 90% to 92% of the phase ( $p = 0.049$ , mean significant Cohen's  $d = 0.513$ ; Fig. 3C).

### 3.3. Muscle–tendon function

Group mean MTU, fascicle, and tendinous tissue lengths during jumping for the non-blocked and blocked conditions are depicted in Fig. 4, and group mean MTU and fascicle velocities are presented in Fig. 5. There were no significant differences in MG fascicle length (Fig. 4A) or MG MTU length (Fig. 4C) between conditions. Participants jumped with

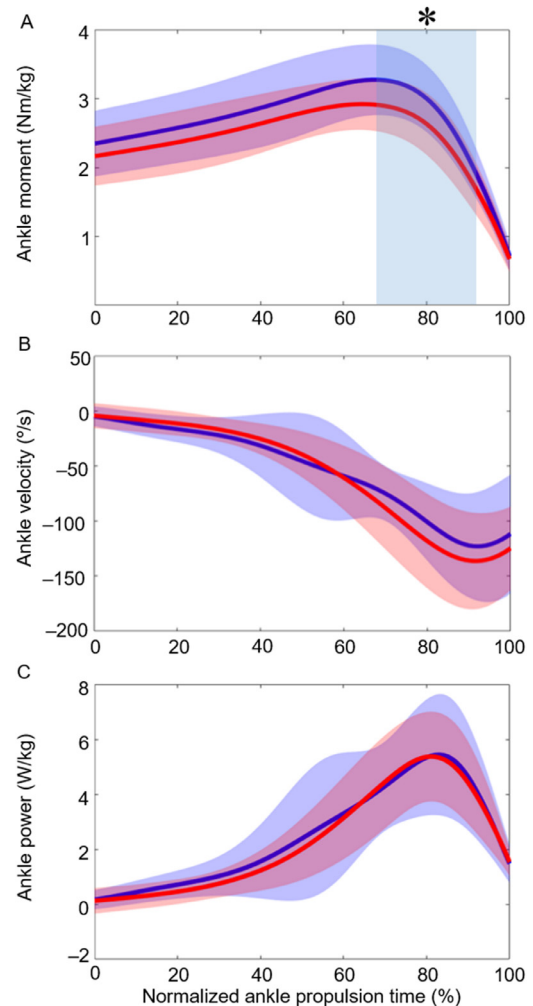


Fig. 2. Group mean data ( $n = 14$ ) for (A) ankle moment, (B) ankle velocity, and (C) ankle power in both non-blocked (blue) and blocked (red) conditions during jumping. All data are time normalized to the mean trial length from the bottom of the countermovement to 25% of peak vertical ground reaction force. Regions of percent-time with shading and asterisk to represent statistically significant differences between conditions ( $p \leq 0.05$ ).

shorter tendon lengths in the blocked condition from 42% to 100% of the propulsive phase ( $p < 0.001$ , mean significant Cohen's  $d = 0.138$ ; Fig. 4B). No significant differences in MG MTU (Fig. 5A) or fascicle (Fig. 5B) shortening velocities were observed between conditions.

Fig. 6 shows the filtered, time-normalized, and enveloped EMG for the MG and TA muscles during the propulsion phase of jumping. For the MG, activity appears slightly higher throughout propulsion in the non-blocked condition, but there were no significant changes in activation between conditions. For TA activity, both conditions display a similar pattern of consistent activation throughout, and there were no significant differences in the magnitude of activation between conditions.

## 4. Discussion

In this study, we explored the influence of the IFM on ankle joint mechanics and ankle plantar flexor function during maximal effort vertical unilateral jumping. We applied a peripheral

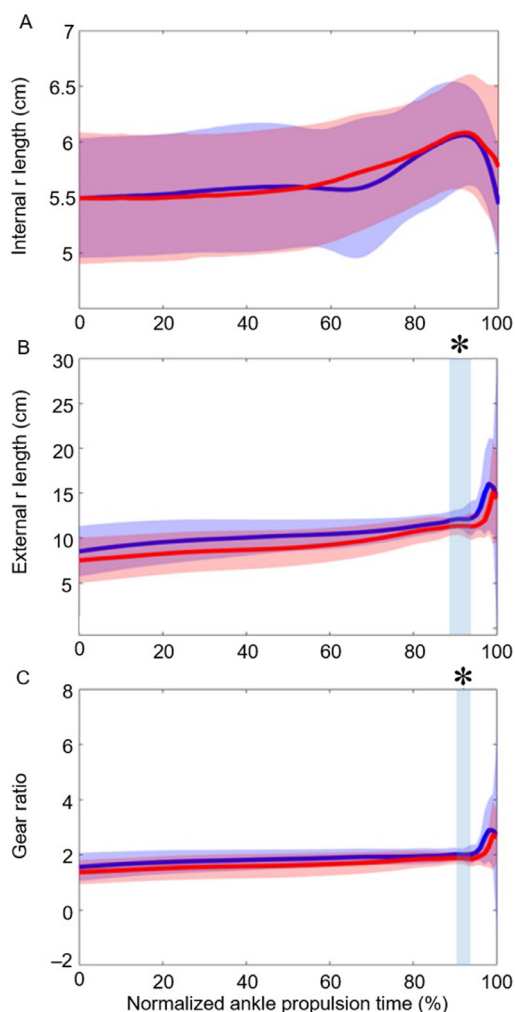


Fig. 3. Group mean data ( $n = 14$ ) for (A) internal moment arm ( $r$ ) length, (B) external  $r$  length, and (C) gear ratio in both non-blocked (blue) and blocked (red) conditions during jumping. All data are time normalized to the mean trial length from the bottom of the countermovement to 25% of peak vertical ground reaction force. Regions of percent-time with shading and asterisks represent statistically significant differences between conditions ( $p \leq 0.05$ ).

nerve block to selectively anaesthetize the plantar IFM, temporarily preventing these muscles from actively producing force, thus allowing us to determine their influence by eliminating their contributions. In line with our hypothesis, we observed a reduction in the external moment arm length and ankle joint moment in the presence of the nerve block. This occurred alongside a reduction in MTPj stiffness and vertical jump height. Despite the changes in ankle joint mechanics, MG muscle contractile dynamics remained relatively constant across both conditions. These findings suggest that the IFM directly affect ankle joint mechanics by actively controlling the leverage of the foot during propulsion.

The external ankle joint moment arm length was shorter when the IFM could not actively tune the stiffness of the MTPj. Previous work from our lab has suggested that the IFM may act to control the center of pressure underneath the foot and, therefore, the ankle's external moment arm.<sup>19,33</sup> Our data

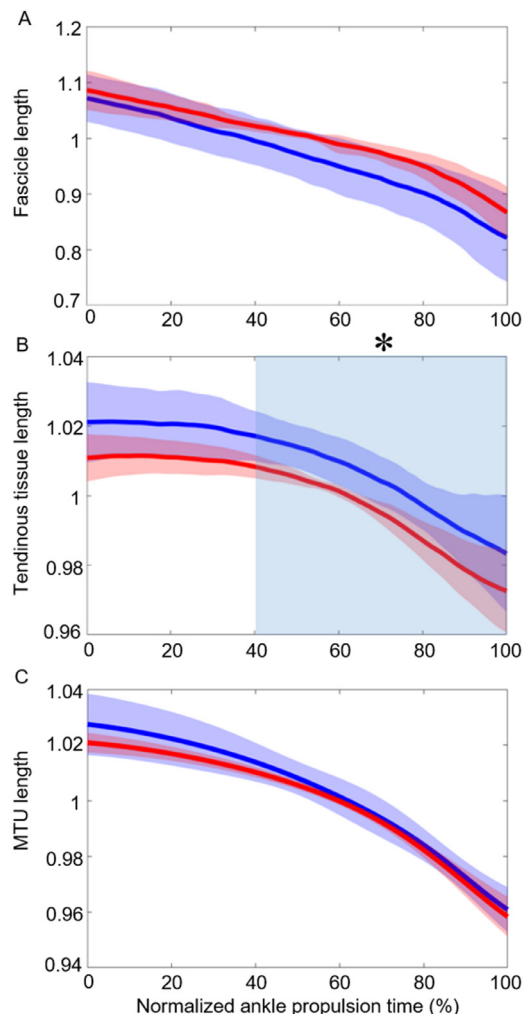


Fig. 4. Group mean data ( $n = 12$ ) for (A) fascicle length, (B) tendon length, and (C) muscle–tendon unit (MTU) length in relation to mean non-blocked-condition length in both non-blocked (blue) and blocked (red) conditions during jumping. All length changes are represented as a percentage of mean length per variable and were divided by the same normalizing value for both conditions. Data are time normalized to the mean trial length from the countermovement bottom to 25% of peak vertical ground reaction force. Region of percent-time with shading and asterisk represent statistically significant differences between conditions ( $p \leq 0.05$ ).

show that during jumping propulsion, the IFM act at the MTPj to plantar flex the toes (push into the ground), creating an anterior shift in the center of pressure and lengthening the external moment arm during late propulsion. These findings also appear to reinforce the concept, suggested by Mann and Inman<sup>36</sup> and Farris et al.,<sup>10,11</sup> that the role of the IFM during locomotor propulsion is to stiffen the forefoot and improve leverage.

A less-stiff foot under the nerve block may explain some of the decrement in ankle moments observed, where 1 could consider the foot to be the “resistance” to ankle plantar flexion during propulsion. While the decrease in external moment arm lengths could explain the decrease in ankle moments in the blocked condition, we only detected significant differences at the end of the propulsion phase. In contrast, the ankle moment was reduced throughout propulsion. It is difficult to ascertain

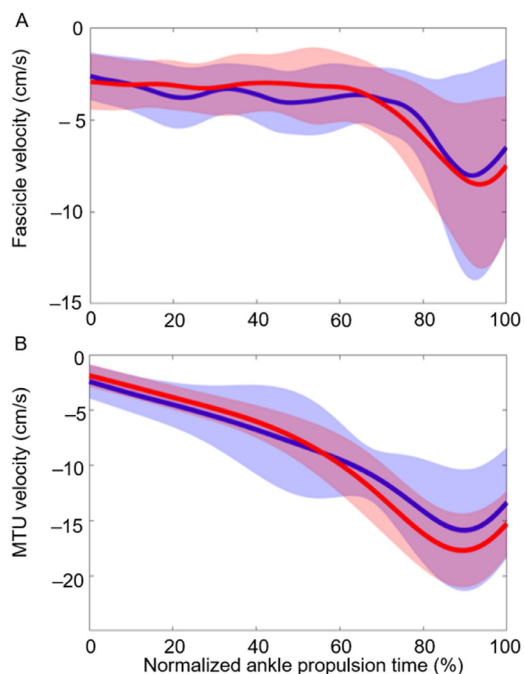


Fig. 5. Group mean data ( $n=12$ ) for (A) fascicle velocity and (B) muscle–tendon unit (MTU) velocity in both non-blocked (blue) and blocked (red) conditions during jumping. All data are time normalized to the mean trial length from the bottom of the countermovement to 25% of peak vertical ground reaction force. Negative velocity values are indicative of shortening.

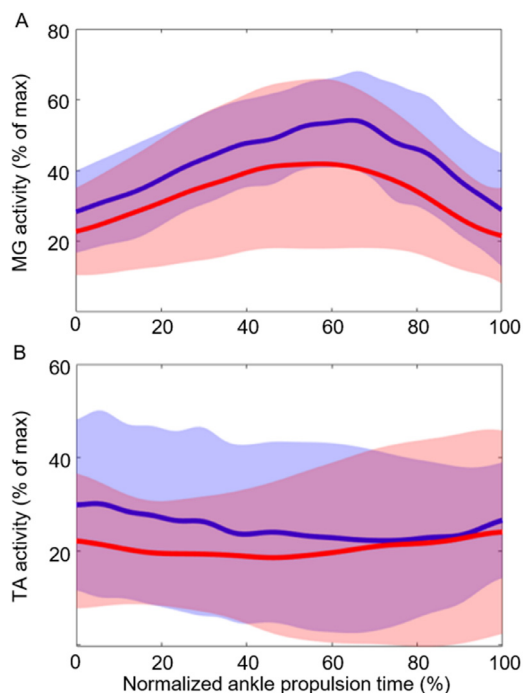


Fig. 6. Group mean data ( $n=14$ ) for (A) medial gastrocnemius (MG) muscle activity and (B) tibialis anterior (TA) muscle activity in both non-blocked (blue) and blocked (red) conditions during jumping. All data are time normalized to the mean trial length from the bottom of the countermovement to 25% of peak vertical ground reaction force.

whether there may have been changes in muscle force with the nerve block. While we saw no change in MG muscle activation or fascicle dynamics, there were decreases in the MG tendinous tissue length, suggesting lower forces generated by the MG. This also aligns with the finding of reduced ankle moment, which is discussed in detail below. A combination of reduced muscle force generation and changes in external moment arm therefore likely contributed to the reduced ankle moment in the blocked condition. The reduced ankle moment was also likely a contributing factor to the lower vertical ground reaction force seen in the blocked condition.

In contrast to previous reports on running<sup>10</sup> and landing and submaximal jumping,<sup>12</sup> we saw no changes in ankle power between conditions during jumping propulsion. Mechanically, if the ankle joint moment is decreased and ankle joint velocity is unchanged, the power would necessarily decrease. This appears to be a result of statistical resolution, as the greater variability observed for ankle joint velocity may have negatively impacted the test's ability to detect a difference in ankle power, considering that the moment was significantly decreased under the block.

Contrary to our hypothesis, the reduction in ankle joint moments was not driven by changes in MG muscle fascicle dynamics. Takahashi et al.<sup>8</sup> found that by adding stiffness to the foot/shoe complex, soleus fascicle velocities increased while soleus force output increased. The goal of our experimental design was to invert this stiffness manipulation (i.e., reduce foot stiffness with the nerve block) to impose unfavorable MG fascicle velocity and force conditions. While our nerve block did decrease MTPj quasi-stiffness, the range of longitudinal bending stiffnesses employed by Takahashi et al.<sup>8</sup> was larger than that of our experimental manipulations (22.5–65.6 N/mm). While rotational joint quasi-stiffness and linear longitudinal bending stiffness are not directly comparable, the differences in magnitudes of imposed stiffnesses between projects may explain why soleus fascicles were more greatly affected during walking propulsion than MG fascicles were during jumping propulsion. Additionally, we only collected ultrasound data from the MG. It is possible that the lateral gastrocnemius or soleus muscle fascicles may have behaved in a different manner during jumping in order to drive the observed increases in ankle moments. Throughout the entirety of the propulsive phase, MG fascicle lengths were subtly longer (2–3 mm) and tendinous tissue lengths significantly shorter (3–5 mm) in blocked condition for the last 60% of propulsion. The reductions in tendinous tissue length—and hence, the likely reduction in MG force—are presumably driven by subtle changes in kinematics and kinetics that impact MTU dynamics and force producing ability. So, while the nerve block did not affect MG fascicle velocities, the IFM appear to play a role in ankle plantar flexor MTU dynamics, particularly in relation to the production of ankle moments.

Of note, peak force production in the blocked condition occurred earlier than in non-blocked condition. As propulsion times were similar between conditions, this may indicate greater peak power production in the nonblocked condition and explain the 2-cm reduction in jump height under the block. However, net vertical impulse (impulse during propulsion

minus body weight, divided by body mass) was similar between conditions (blocked =  $145 \text{ N} \times \text{s}$ , non-blocked =  $148 \text{ N} \times \text{s}$ ), which is an observation that has been used to explain jump height differences in previous literature.<sup>37</sup> Rather, we found that for the majority of participants, COM position just before take-off was higher in the nonblocked jumps than the blocked jumps, such that similar impulse was generated, but jump height was higher for the nonblocked conditions only as a result of a higher position at take-off. Therefore, it seems that subtle changes in joint kinematics under the block led to different take-off positions during jumping that influenced our jump height measures.

This study has several limitations. The first is the decreased sample size after the exclusion of 2 participants' muscle fascicle data. When reporting MTPj stiffness, we applied an average linear slope to reflect the rotational stiffness, or quasi-stiffness, of the MTPj. Of note, this relationship was not perfectly linear across participants (Supplementary Fig. 1), but, given the large difference in magnitude of effect between conditions, we are confident that the reported method adequately reflects the effect of the nerve block on MTPj quasi-stiffness. Our measure of internal moment arm length was an estimate based on kinematic data, not direct measurement. Another limitation is the unilateral jumping task, which was chosen to allow only a single foot to be injected with local anesthesia. This was required to ensure the legally (and safe) permitted dosage of local anesthetic for a nerve block (3 mg/kg of body mass) was applied to only a single foot, thereby maximizing the efficacy of the intervention. The performance of the unilateral task then has a balance component that is not present in other maximal-effort tasks, which may result in alterations of the mechanics or joint contributions required to perform jumps. Due to these balance constraints, we allowed the use of arm swing, which is well established to aid in jumping performance. Thus, some participants may have demonstrated greater ability to influence jumping performance by utilizing arm swing, but we were not able to quantify this potential contribution. Also, greater arm swing might be used to maximize jump performance in the presence of the block. Therefore, if this was to be a confounder, it may actually mean that our effects would be larger than reported here. Also, although maximal efforts were encouraged, the block may have led to a feeling of instability when jumping or landing, which could influence neural drive. In addition to blocking recruitment of the IFM, the nerve block also removes sensation from the plantar foot surface. Therefore, it is plausible that mean ankle moments decreased due to lack of feedback between the central nervous system and the muscle. We would then anticipate altered muscle activity due to disruptions in excitatory or inhibitory input on the MG's motor neuron pool. This was not the case for our data, which we believe provides sound rationale that the alterations observed here are mechanical in nature. However, this explanation assumes similar activation behavior for the other muscles that plantarflex the ankle. As our study did not collect muscle activity or fascicle imaging data for the soleus or lateral gastrocnemius, we cannot completely rule out sensory influences imposed by the block.

## 5. Conclusion

We have provided direct evidence of mechanical coupling between the IFM and the ankle joint. In addition to their known role of regulating the energetic function of the foot, these muscles also have the capacity to alter the leverage function of the foot and ankle joint moment production during propulsion.

## Acknowledgments

This work was funded by an Australian Research Council Linkage Grant (LP160101316), in collaboration with Asics Oceania and The Australian Sports Commission. The funding source had no involvement with the study design, data collection, data processing, manuscript writing or editing, or the decision to submit this manuscript.

## Authors' contributions

GL, DF, and LK participated in the design of the study; RS contributed to data collection. All authors contributed to data reduction/analysis, interpretation of results, and manuscript writing. All authors have read and approved the final version of the manuscript, and agree with the order of presentation of the authors.

## Competing interests

The authors declare that they have no competing interests.

## Supplementary materials

Supplementary material associated with this article can be found in the online version at doi:10.1016/j.jshs.2022.07.002.

## References

1. Farris DJ, Sawicki GS. The mechanics and energetics of human walking and running: A joint level perspective. *J R Soc Interface* 2012;**9**:110–8.
2. Ishikawa M, Komi PV, Grey MJ, Lepola V, Brüggemann GP. Muscle–tendon interaction and elastic energy usage in human walking. *J Appl Physiol* (1985) 2005;**99**:603–8.
3. Lichtwark GA, Bougoulas K, Wilson AM. Muscle fascicle and series elastic element length changes along the length of the human gastrocnemius during walking and running. *J Biomech* 2007;**40**:157–64.
4. Carrier DR, Heglund NC, Earls KD. Variable gearing during locomotion in the human musculoskeletal system. *Science* 1994;**265**:651–3.
5. Erdemir A, Piazza SJ. Rotational foot placement specifies the lever arm of the ground reaction force during the push-off phase of walking initiation. *Gait Posture* 2002;**15**:212–9.
6. Baxter JR, Novack TA, Van Werkhoven H, Pennell DR, Piazza SJ. Ankle joint mechanics and foot proportions differ between human sprinters and non-sprinters. *Proc Biol Sci* 2012;**279**:2018–24.
7. Lee SS, Piazza SJ. Built for speed: musculoskeletal structure and sprinting ability. *J Exp Biol* 2009;**212**:3700–7.
8. Takahashi KZ, Gross MT, Van Werkhoven H, Piazza SJ, Sawicki GS. Adding stiffness to the foot modulates soleus force-velocity behaviour during human walking. *Sci Rep* 2016;**6**:29870. doi:10.1038/srep29870.
9. Willwacher S, König M, Braunstein B, Goldmann JP, Brüggemann GP. The gearing function of running shoe longitudinal bending stiffness. *Gait Posture* 2014;**40**:386–90.



10. Farris DJ, Kelly LA, Cresswell AG, Lichtwark GA. The functional importance of human foot muscles for bipedal locomotion. *Proc Natl Acad Sci U S A* 2019;**116**:1645–50.
11. Farris DJ, Birch J, Kelly L. Foot stiffening during the push-off phase of human walking is linked to active muscle contraction, and not the windlass mechanism. *J R Soc Interface* 2020;**17**: 20200208. doi:10.1098/rsif.2020.0208.
12. Smith RE, Lichtwark GA, Kelly LA. The energetic function of the human foot and its muscles during accelerations and decelerations. *J Exp Biol* 2021;**224**:242263. doi:10.1242/jeb.242263.
13. Kelly LA, Cresswell AG, Farris DJ. The energetic behaviour of the human foot across a range of running speeds. *Sci Rep* 2018;**8**:10576. doi:10.1038/s41598-018-28946-1.
14. Riddick R, Farris DJ, Kelly LA. The foot is more than a spring: Human foot muscles perform work to adapt to the energetic requirements of locomotion. *J R Soc Interface* 2019;**16**:20180680. doi:10.1098/rsif.2018.0680.
15. Unger CL, Wooden MJ. Effect of foot intrinsic muscle strength training on jump performance. *J Strength Cond Res* 2000;**14**:373–8.
16. Yuasa Y, Kurihara T, Isaka T. Relationship between toe muscular strength and the ability to change direction in athletes. *J Hum Kinet* 2018;**64**:47–55.
17. Hashimoto T, Sakuraba K. Strength training for the intrinsic flexor muscles of the foot: Effects on muscle strength, the foot arch, and dynamic parameters before and after the training. *J Phys Ther Sci* 2014;**26**:373–6.
18. Goldmann JP, Sanno M, Willwacher S, Heinrich K, Brüggemann GP. The potential of toe flexor muscles to enhance performance. *J Sport Sci* 2010;**31**:424–33.
19. Kelly LA, Cresswell AG, Racinais S, Whiteley R, Lichtwark GA. Intrinsic foot muscles have the capacity to control deformation of the longitudinal arch. *J R Soc Interface* 2014;**11**:20131188. doi:10.1098/rsif.2013.1188.
20. Leardini A, Benedetti MG, Berti L, Bettinelli D, Nativo R, Giannini S. Rear-foot, mid-foot and fore-foot motion during the stance phase of gait. *Gait Posture* 2007;**25**:453–62.
21. van den Bogert AJ, Su A. A weighted least squares method for inverse dynamic analysis. *Comput Methods Biomech Biomed Engin* 2008;**11**:3–9.
22. Lu TW, O'Connor JJ. Bone position estimation from skin marker co-ordinates using global optimisation with joint constraints. *J Biomech* 1999;**32**:129–34.
23. Brennan SF, Cresswell AG, Farris DJ, Lichtwark GA. *In vivo* fascicle length measurements via B-mode ultrasound imaging with single vs. dual transducer arrangements. *J Biomech* 2012;**64**:240–4.
24. Wakeling JM, Jackman M, Namburete AI. The effect of external compression on the mechanics of muscle contraction. *J Appl Biomech* 2013;**29**:360–4.
25. Bruening DA, Takahashi KZ. Partitioning ground reaction forces for multi-segment foot joint kinetics. *Gait Posture* 2018;**62**:111–6.
26. Day EM, Hahn ME. A comparison of metatarsophalangeal joint center locations on estimated joint moments during running. *J Biomech* 2019;**86**:64–70.
27. Dempster WT. *Space requirements of the seated operator: Geometrical, kinematic, and mechanical aspects of the body with special reference to the limbs*. Ann Arbor, MI: University of Michigan; 1955.
28. Hanavan EP. A mathematical model of the human body. *AMRL TR* 1964:1–149.
29. Hawkins D, Hull ML. A method for determining lower extremity muscle-tendon lengths during flexion/extension movements. *J Biomech* 1990;**23**:487–94.
30. Farris DJ, Lichtwark GA. UltraTrack: Software for semi-automated tracking of muscle fascicles in sequences of B-mode ultrasound images. *Comput Methods Programs Biomed* 2016;**128**:11–8.
31. Cronin NJ, Carty CP, Barrett RS, Lichtwark GA. Automatic tracking of medial gastrocnemius fascicle length during human locomotion. *J Appl Physiol (1985)* 2011;**111**:1491–6.
32. Kurokawa S, Fukunaga T, Fukashiro S. Behavior of fascicles and tendinous structures of human gastrocnemius during vertical jumping. *J Appl Physiol (1985)* 2001;**90**:1349–58.
33. Kelly LA, Kuitunen S, Racinais S, Cresswell AG. Recruitment of the plantar intrinsic foot muscles with increasing postural demand. *Clin Biomech (Bristol, Avon)* 2012;**27**:46–51.
34. Pataky TC. Generalized n-dimensional biomechanical field analysis using statistical parametric mapping. *J Biomech* 2010;**43**:1976–82.
35. Reddan MC, Lindquist MA, Wager TD. Effect size estimation in neuroimaging. *JAMA Psychiatry* 2017;**74**:207–8.
36. Mann R, Inman VT. Phasic activity of intrinsic muscles of the foot. *J Bone Joint Surg Am* 1964;**46**:469–81.
37. Kirby TJ, McBride JM, Haines TL, Dayne AM. Relative net vertical impulse determines jumping performance. *J Appl Biomech* 2011;**27**: 207–14.